# Influence of Cu Addition to Improve Shape Memory Properties in NiTi Alloys Developed by Laser Rapid Manufacturing

S. Shiva[*1], I. A .Palani[*1*2], S. K. Mishra[*3], C. P. Paul[*3] and L. M. Kukreja[*3]

[*1] *Laser Mechatronics and Instrumentation Laboratory, Indian Institute of Technology, Indore 453441, India*
*E-mail: sshivabemech@gmail.com*
[*2] *Centre for Material Science and Engineering, Indian Institute of Technology Indore 453441, India*
[*3] *Laser Materials Processing Division, Raja Ramanna Centre for Advanced Technology, Indore, 452013, India*

In recent times Ni-Ti shape memory alloy flaunts exceptional outputs in the line of MEMS, serving as actuators. An attempt has been successfully made to develop Ni-Ti structures using laser rapid manufacturing (LRM). However the occurrence of brittleness was a drawback in the attempt. As a remedial measure Cu is included along the binary alloy to form a ternary alloy. Also the inclusion of Cu has an advantage of low hysteresis generation during phase transformations. Developing NiTiCu shape memory alloy by additive manufacturing is a novel approach for this work. The substitution of Cu with Ni can be up to 15 wt% to 30 wt% to possess shape memory properties[1]. In the current investigation combination of Ti50% Ni25% Cu25% alloy formation has been done and it is represented as NiTiCu25. Investigations were carried out to determine the product's surface morphology, phase transformation temperature, crystalline nature through scanning electron microscopy (SEM), differential scanning calorimetry (DSC) and x-ray diffraction (XRD) respectively. These results are compared with equiatomic Ni-Ti which has been manufactured using LRM. From the investigations it was observed that the inclusion of Cu gives improved surface texture and multiple phase peaks in XRD. Also the heat flow curves which had steep peaks in DSC analysis, indicate the presence of phase transformations in the samples fabricated using LRM.

DOI: 10.2961/jlmn.2016.02.0003
**Keywords:** laser rapid manufacturing, SEM, XRD, DSC, NiTiCu alloy

## 1. Introduction

The shape memory alloy (SMA) owns a special place in the line of micro electro mechanical systems (MEMS) in the role of actuators. Widely the MEMS applications have started relying on SMAs due to the nature of functioning during their deformed state. Most interestingly their shape memory nature brings them back to their original shape, in case of two way shape memory effect. This is achievable due to their phase transformation capabilities [2-5]. The ability of the material to retain its shape is possible only if the alloys have a good twinning and detwinning ability in its lattice structure and this is possible through good bonding of elements among themselves. So the challenge awaits in manufacturing these alloys with a find bond between the elements, to obtain its shape memory effects. Among the several shape memory alloys available in practice Ni-Ti has placed itself to be in the first choice, with its stability in shape memory nature and its long life in exhibiting the shape memory effect [6, 7]. When altering the alloy with the inclusion of Cu, researchers have proved the shape memory nature remains the same when the Cu wt% lies between 15-30 wt% [8]. The manufacturing of Ni-Ti shape memory alloy has been successfully proven by several process [9-11]. However laser rapid manufacturing is a new novel methodology for manufacturing NiTiCu tailor made structures.

In this work a comparative study between equiatomic NiTi50 and NiTiCu25 has been carried out. The work includes the surface morphology studies, microstructural analysis, micro-hardness measurement and shape memory effect analysis. Particularly the inclusion of Cu in and their effect regarding shape memory effects have been investigated.

The properties of the as fabricated NiTiCu25 structures developed using laser based rapid manufacturing have been investigated in detail.

## 2. Experimental Procedure

A 2 kW fiber laser based rapid manufacturing (LRM) system [12] was deployed for laser rapid manufacturing of various deposits involving Ni and Ti. As shown in fig.1 the laser system is connected to a five axis workstation in a glove box. A computerized numerical controller controls the entire operation. Coaxial nozzles were used to feed the powder for developing the samples, from a twin powder feeder. The laser beam was transferred to 5-axis CNC laser workstation through an optical fiber and a quartz lens (focal length = 200 mm) to focus the beam at the laser workstation [13]. A defocused beam of diameter about 2 mm was delivered on the substrate surface along the powder to develop the samples on the substrate. Pure Ti plate of size 100 mm x 100 mm x 8 mm thick was used as substrate. Titanium substrate is being used in this experiment expect-

ing an easy debonding, as the thermal expansion coefficients are different for Ni-Ti and Ti [12]. Prior to the experiments, the substrates were sand-blasted to roughen the machined surface so as to increase the laser absorption. The purity of the powders used were 99.9% of grain size of 45-106 µm. The powders were pre mixed with a table top powder mixer before being fed into the hopper. Argon gas was used as shielding and carrier gas [14], which passes through the powder feeder, containing the pre mixed powder to transfer it into the work station inside the shielded chamber for generating the samples. The fabricated structures were let to cool inside the argon shielded casing, under the same atmospheric conditions used for fabrication.

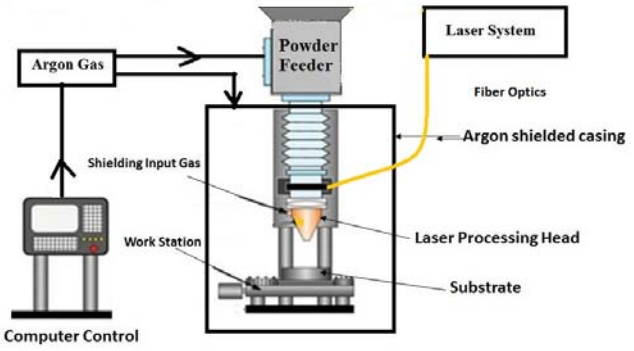


**Fig. 1** Schematic diagram of LRM setup.

In fig.2 the as made sample of NiTi50 can be seen. Similar sample of TiNiCu25 were also made. The scanning speed was consistently maintained at 10-14 mm/sec. Each track was developed at 1 mm in width. Using the same plot several tracks were deposited in order to obtain a thin film structure. The deposited film structure was of dimension 90 mm in length and 10mm in width and 1.5 mm in thickness. The final product was of dimension 70 mm X 10 mm X 1 mm after some part of it was trimmed using wire electrical discharge machining (EDM). The final product was made to undergo various characterizations in order to study its surface morphology, mechanical properties, and crystalline nature and phase transformation effects.


**Fig. 2** Sample developed by LRM

The surface morphological analyses of the samples were carried out using scanning electron microscopy (Zeiss, Model: Supra55) attached with Energy dispersive spectrograph (Oxford Instruments, Model: X-mas). Surface roughness measurements were investigated using optical profilometer (Veeco NT9080). Microstructure analyses was done using optical microscope (Leica DFC295). The structural analysis was carried out by X-ray diffractor (Rigaku Model: Smart lab Automated Multipurpose). The shape memory effect was characterized using Differential Scanning Calorimetry (TA Instruments, Model: DSC 2910). The micro-hardness of the samples were measured using micro-hardness testing machine (UHL, Model: VMH 002).

## 3. Results and Discussion

### 3.1 Surface Morphology and microstructure

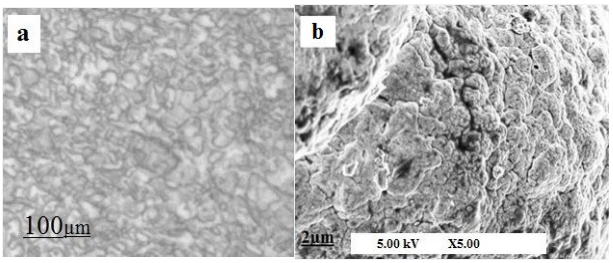


**Fig. 3** Image of NiTi50 (a) Microstructure (b) SEM.

Characterizations have been done on samples prepared in the similar manner in which good results have been obtained previously in our initial attempt [15]. In Fig. 3 the surface morphology and microstructure of NiTi50 is shown. Fig. 3(a) shows the microstructure of the sample to be uneven but the particles are close in bond. Presence of mild cracks on the surface is not clearly observed at this level (Magnification of 5.00 KX and acceleration Voltage of 5.00KV) as shown in Fig 3(b). The presence of carbon and oxygen can cause mild cracks on the surface as reported by researchers in the past [16]. Also the presence of a mild layer of oxidation is common when NiTi is fabricated using laser interaction [16]. Those effects can be seen in fig 3(b) as the surface is not so even and dents and cracks are mildly found. Generally negligible amount of C and O are in built residues in the powders when they are manufactured [17]. By the inclusion of copper the problems of inbuilt C and O can be overcome. As copper is a metal which can react with these negligible amounts of C and O and convert them to vapor which will be absorbed by the argon atmosphere [17]. The surface roughness values of NiTi50 and NiTiCu25 are measured to be 3.12 µm and 3.14 µm respectively.

Parallely Energy Dispersive Spectroscopy (EDS) was carried out for both samples and they are quoted in the following Table 1. The EDS shows Ni-50.23% and Ti-49.77% in for NiTi50 combination. Our early works also showed some increase in the wt% of nickel. Reason behind the increase in Ni weight percentage is due to the formation of NiTi2 phases in the alloy [18]. For NiTiCu25 it is observed Ni-35.23%, Ti-49.32% and Cu-15.45%. So the inclusion of Cu and its capability of blending with Ni and Ti is clearly

**Table 1** EDS Results of the samples

| Material | NiTi50 | NiTiCu25 |
|---|---|---|
| Ti | 49.77 Wt % | 49.32 Wt % |
| Ni | 50.23 Wt % | 35.23 Wt % |
| Cu | - | 15.45 Wt % |

visualized as the percentage of Cu has considerably reduced resulting in the formation of (NiCu) Ti. Now the alloy formation using this method is confirmed so further examination is to be done to find its crystalline nature and phase transformation capabilities.

In fig 4 the microstructure and SEM of both the samples are shown. The grain size in fig. 4(a) of NiTiCu25 sample seems to be smaller than NiTi50 and as a result in fig. 4(b) the SEM image shows a smooth surface without any island structures. This has been confirmed by the calculated grain size using scherrer's formula in section 3.3 too. Visually both samples are densely packed and cracks or porosity holes are not seen. The rigidity of the material can be found by micro-hardness tests and those results will confirm the homogeneity of deposition. If the homogeneity is confirmed to be good this methodology of laser rapid manufacturing will earn more credits in the aspect of fine manufacturing process.

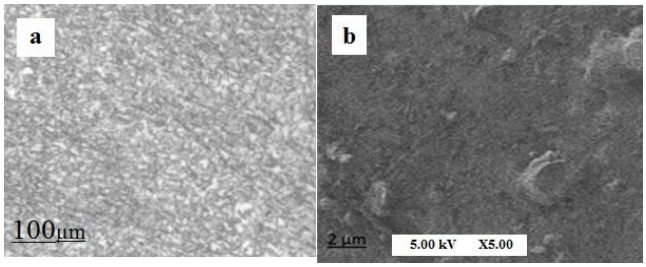


**Fig. 4** Image of NiTiCu25 (a) Microstructure (b) SEM.

Fig. 5 shows the micro-hardness and the standard deviation of the samples. The samples made by laser rapid manufacturing were cut transverse to the direction of laying and prepared using standard metallographic techniques and micro-hardness measurement was carried out at an incremental distance of 25 µm at a load of 500 g. Ten readings were taken and the average value of micro-hardness was found to be 388 and 395 HVN for NiTi50 and NiTiCu25 respectively. The standard deviation limit is also quite equal for both the samples. The less amount of standard deviation proves the deposition of the materials have been uniform throughout the experiments and the absence of porosity.

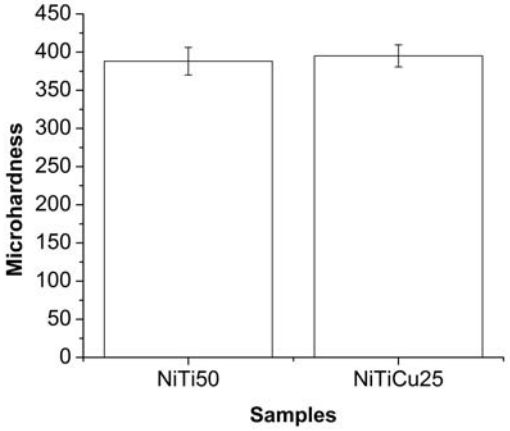


**Fig. 5** Micro-hardness and standard deviation of formed samples

### 3.2 Mechanical Properties

To investigate the mechanical properties of the formed samples, standard tensile test samples of ASTM standards in the dimensions as shown in Fig. 6 were fabricated individually and the tests were conducted. The tensile strength and the corresponding modulus measurements obtained from the formed samples are quoted in Table 2. From Fig. 7, results it's very vivid that the elasticity of the materials formed are low due to their brittle nature, and all the three samples are comparatively uniform. As the percentage of Ti increases in the alloy, the elasticity gradually decreases. The amount of ultimate tensile strength increases as the percentage of Ni increases in the alloy.

**Table 2** Mechanical Propeties of the materials

| Material | NiTi50 | NiTiCu25 |
|---|---|---|
| Young's Modulus (GPa) | 19 | 23 |
| Ultimate strength (MPa) | 319 | 336 |

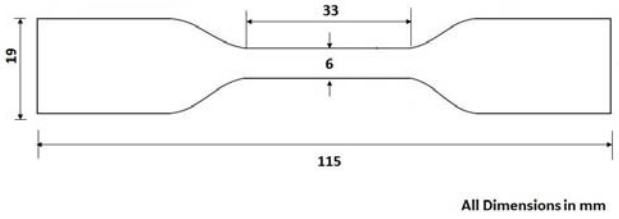


**Fig. 6** Diagram of UTM test sample.

The tensile strength and the Young's modulus values are tabulated in Table I. Fig. 7, shows the stress strain curves of both the samples. In equiatomic composition, the elasticity gradually decreases. Where as in the ternary alloy the Young's modulus has a slight increment indicating the effect of Cu in the composition. The amount of ultimate tensile strength increases as Ni blends with Cu in the alloy of NiTiCu25 than NiTi50.

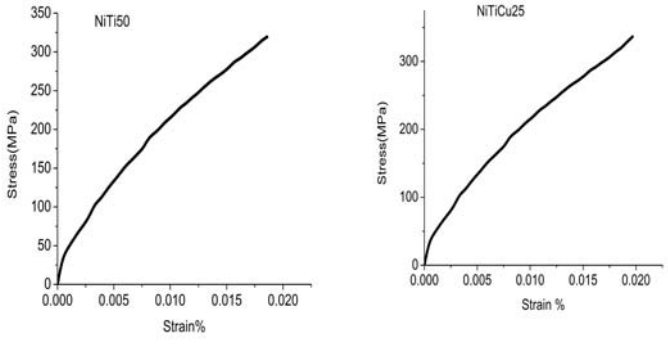


**Fig. 7** Stress Vs Strain graphs of the samples

While comparing ultimate strength of both the samples the Cu mixed samples have higher ultimate strength and this is achieved by the impact of Cu. The element Cu acts as a good binder of NiTi together and it leads to the formation of good quality of shape memory alloy in the aspect of ductility and low hysteresis which is good for its effective shape recovery capability. This can also be seen in our forth coming DSC tests results. As of our comparison NiTi50 and NiTiCu25 manufactured by laser rapid manufacturing have produced good stress strain curves and the ternary alloy NiTiCu25 displays some better results than the binary alloy NiTi50. This is an additional advantage in the prospect of good shape memory properties with enough ductility.

### 3.3 Structural Characteristics

The formed samples were cut using wire EDM in a dimension of 1 mm width, 1mm breadth and 1mm thickness for performing the XRD test. In Fig. 7, the XRD peaks of NiTi50 reveals the presence of martensite phase at 2θ= 40º3' in monoclinic structure and the austenite phase takes a high peak at 2θ= 43º45', in which the material remains in cubic structure. Even a small change in the Ni content of the Ni-Ti alloy can give a large difference in its properties. The result of NiTiCu25 in Fig. 8 proves the peaks can be obtained without any variation in the standard Ni-Ti peak. It has its martensite peak B19' at 2θ= 39º75' and austenite peak B2 only up to a remarkable elevation at 2θ= 43º75' as shown. The presence of two phases austenite and martensite are vivid. The patterns of these formed samples have peaks which are broad, which clearly intimates that, the grain structure of the two samples formed are very small, especially NiTiCu25 [19]. That is the reason for its wider peak than NiTi50. Crystallite size can be calculated by measuring the Bragg peak width at half the maximum intensity and using the Scherrer formula:

$$d = \frac{0.9\lambda}{BCos\theta} \quad (1)$$

Where d is for crystallite size, λ stands for wavelength of the X-Ray radiation used, B is the peak width at half the intensity, and θ is the Bragg angle [20] the crystallite size calculated using Scherrer formula is 34.81nm and 30.31nm.

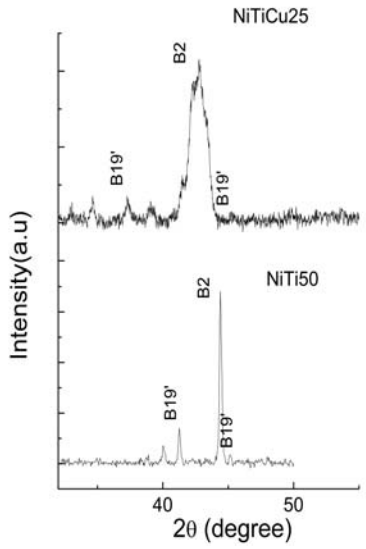


**Fig. 7** XRD graphs of the samples

### 3.4 Shape Memory Characteristics

Fig. 9 shows the DSC curves of the formed samples. Both the combinations show the phase transformation curves visible in both heating as well as cooling. In fact NiTiCu25 has steep curves than the NiTi50. This is a clear indication, confirming the presence of good shape memory characteristics in the formed samples. For NiTi50 the austenite start temperature ($A_s$) is at 2.5 ºC and austenite finish temperature ($A_f$) is at 21 ºC. The martensite start temperature ($M_s$) = 5 ºC and parallely martensite finish temperature ($M_f$) = -15 ºC are clearly visible in the plot, this is, due to the proper lattice structure. NiTiCu25 has its $M_s$ = 58 ºC and $M_f$ = 42 ºC similarly As = 54 ºC and $A_f$ = 80 ºC. $A_s$ and $A_f$ are the corresponding temperatures for the reverse transformation from B19' to B2. Hysteresis is another factor to be considered for a good phase transformation process as minimizing the hysteresis maximizes the transformation. The hysteresis of NiTiCu sample seems to be less as they should be, from the obtained phase transformation temperatures. The DSC curves give more confirmation along with XRD graph that NiTiCu samples can be successfully made with no reduction in the shape memory characteristics of the material.

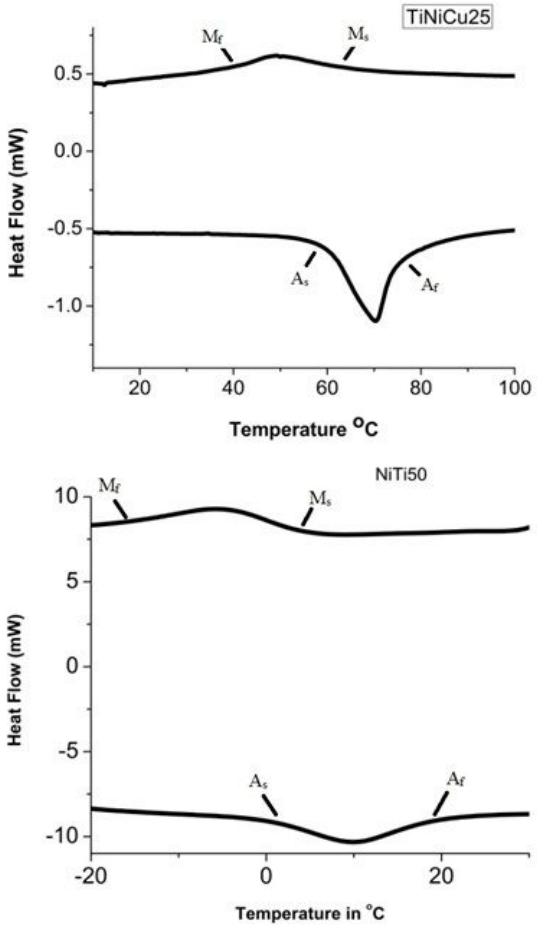


**Fig. 9** DSC graphs of the Samples

From all the characterizations done and the results obtained it can now be assured the process of developing NiTiCu through laser rapid manufacturing, a successful one. SEM and EDS assures the quality of the produced materi-

als in the prospect of good alloy formation. The surface morphology of NiTiCu25 was comparatively smoother. Co-relations were observed between the XRD and DSC graphs. In XRD the presence of secondary phases both in NiTi50 and NiTiCu25 were obtained and the two phase peaks were in the exact position of $2\theta$. But in NiTiCu25 there was a light shift forward due to the impact of microstructure size. In the case of DSC visible phase transformation curves have been obtained for both the samples. The presence of two phases were indicated in XRD graphs and the accurate start and finish temperatures of both the phases were spotted in DSC graphs. The primary requirement for shape memory alloy is the possession of austenite and martensite phases. Once after overcoming the problem of brittleness visual actuation can be expected in the shape memory alloy samples developed by LRM. The most interesting part was for NiTiCu25 results indicating the presence of R phase has been vividly seen. Almost in all the results NiTiCu25 is at par and even better at some cases with NiTi50 including the micro-hardness test.

## 4. Conclusion

In this work the inclusion of Cu along NiTi materials using laser rapid manufacturing has been done. Characterizations were carried out for the formed products. Studies were carried out in determining the particle structure, phase transformations and shape memory effect. Based on the investigations the results obtained are as follows:

(1) Laser rapid manufacturing was a successful method for producing NiTiCu25 materials, without changing their properties of shape memory effect.
(2) The properties of NiTi50 and NiTiCu25 resembled each other.
(3) SEM images and EDS results were convincingly good.
(4) XRD graphs prove NiTiCu25 have also shown some good SMA phase transformation peaks.
(5) DSC graphs confirm the presence of phase transformations for both the NiTi50 and NiTiCu25 samples.
(6) In future to find the best combination of NiTiCu alloys several combinations are to be investigated.

**Acknowledgments**

(1) The authors would like to thank Indian Institute of Technology Indore for assisting us the travel grant to present this paper in LAMP2015 at Fukoka, Japan.
(2) Thanks are also due to Sophisticated Instrument Centre (SIC), Indian Institute of Technology Indore for providing the characterization facilities.

**References**

[1] 0. Mercier and K. N. Melton: Met. Trans. A10 (1979) 387
[2] J. Laeng, Z. Xiu , X. Xu , X. Sun , H. Ru and Y. Liu: Phys.Scr.T., 129, (2007) 250-254.
[3] S.L. Wu, X.M. Liu, P.K. Chu, Chung, C.L. Chu and K.W.K Yeung: J.Alloys Compd., 449, (2008) 139-143.
[4] D.S. Li, Y.P. Zhanng, X . Ma and Zhang: J.Alloys Compd., 474, ( 2009) L1-L5.
[5] S.L. Wu, C.Y. Chung, X.M. Liu, P.K. Chu, J.P.Y. Ho, C.L. Chu,Y.L. Chanc, K.W.K. Yeungc, W.W. Luc, K.M.C. Cheungc and K.D.K. Lukc: Acta Mater., 55, (2007) 3437-3451.
[6] K.E. Wilkes, P.K. Liaw and K.E. Wilkes: JOM., 52, (2000) 45-51.
[7] J. Cederstrom and J. Van Humbeeck: J PHYS III., 5,(1995) C2(335-341).
[8] Ming-Chuan Chen and Shyi-Kaan Wu: Surf Coat Technol., 203,(2009) 1715–1721.
[9] M. Callisti, F.D. Tichelaar, B.G. Mellor and T. Polcar: Surf Coat Technol.,237,(2013) 261-268.
[10] H. J. Zhang and C. J. Qiu: Mater. Trans., JIM., 4, (2006) 532-535.
[11] T. Goryczka and J. Van Humbeeck: JAMME., 17, (2006) 65-68.
[12] P. Bhargava, C.P.Paul, C.H. Premsingh, S.K. Mishra, Atul Kumar, D.C. Nagpure, Gurvinderjit Singh and L. M. Kukreja: Adv. Manuf., 1, (2013) 305–313.
[13] C.P. Paul, P. Bhargava, Atul Kumar, A.K Pathak and L.M Kukreja "Laser rapid manufacturing: technology, applications, modeling and future prospects" by J. Paulo Davim (UK: ISTE-Wiley) p.1-38.
[14] C.P. Paul, P. Ganesh, S.K. Mishra, P. Bhargava, J.Negi and A.K. Nath: Opt Laser Technol., 39,(2007) 800-805.
[15] S. Shiva, I.A. Palani, S.K. Mishra, C.P. Paul and L.M. Kukreja: Opt Laser Technol., 69,(2015) 44-51.
[16] Mohammad H. Elahinia, Mahidi Hashemi, Majid Tabesh and Sarit B.Bhaduri: Progress in Material Science.; 57(2012) 911-946.
[17] S. Sanjabi, Z. H. Barber: Surface and Coatings Tech nology 204 (2010) 1299.
[18] JiangShu-young and Zhang Yan-qiu: Trans.Nonferrous, Met. Soc.China., 22, (2012)90-96.
[19] B.D Cullity, S.R Stock: "Elements of X-Ray Diffraction", 3rd ed. Pearson, 2014.
[20] C. Suryanarayana: progress in Material Science., 46, (2001)1-184.

(Received: May 25, 2015, Accepted: March 16, 2016)